High Float Emulsion Residue: Its Unique Rheology and Microstructure

Justin P. Suda, M.Sc.
Bituminous Binders Chemist
GECAN (a division of Canadian Road Builders Inc.)
Acheson, Alberta

Anthony Yeung, Ph.D., P.Eng.
Professor
Department of Chemical & Materials Engineering
University of Alberta
Edmonton, Alberta

ABSTRACT

Despite the clear benefits of High Float (HF) emulsions, current formulations are not optimized. The design of "next generation" emulsions will require knowledge of the basic science that underlies HF systems. At present, the understanding of HF emulsions is rudimentary in two regards:

- No rheological model is available to predict the flow/deformation of HF materials. The only semi-quantitative characterization is whether the breakthrough time in a float test would exceed 20 minutes.

- The mechanism(s) by which the stabilizer (tall oil soap) gives rise to the unique rheology of HF residues is not understood.

This paper reports a detailed study of the rheology of HF residues. The most notable feature of this material is its yield stress, which can be quantified using a stress-ramp procedure. A rheological model — a hybrid between Bingham fluid and Kelvin-type solid — is developed to predict the ramp response of the residue material. It is proposed that the yield stress, rather than the breakthrough time in float tests, should be the metric for characterizing HF residues and other similar materials. In addition to rheological studies, we speculate also on the microstructure of the HF residue, and how it leads to the material's macroscopic behaviour.

RÉSUMÉ

Malgré les avantages évidents des émulsions HF [High Float], les formulations actuelles ne sont pas optimisées. La conception d'émulsions "nouvelle génération" exigera la connaissance de la science fondamentale qui sous-tend les systèmes HF. À l'heure actuelle, la compréhension des émulsions HF est rudimentaire à deux égards:

- Aucun modèle rhéologique n'est disponible pour prédire le flux/déformation des matériaux HF. La seule caractérisation semi-quantitative est de savoir si le délai de rupture dépasse 20 minutes.

- Les mécanismes par lesquels le stabilisant (savon de tall oil) génère la rhéologie unique des résidus HF ne sont pas compris.

Cet article présente une étude détaillée de la rhéologie des résidus HF. La caractéristique la plus notable de ce matériau est sa limite d'élasticité, qui peut être quantifiée en utilisant une procédure de variation de tension. Un modèle rhéologique - un hybride entre un fluide Bingham et solide de type Kelvin - est développé pour prédire la réponse tension/déformation de la matière résiduelle. Il est proposé que la limite d'élasticité, plutôt que le temps de rupture, devraient être la propriété déterminante pour la caractérisation des résidus de HF et d'autres matériaux similaires. En plus des études rhéologiques, nous émettons une hypothèse quant à la microstructure du résidu HF et comment elle conduit au comportement macroscopique du matériau.

1.0 INTRODUCTION

Pavement preservation refers to the engineering practice that is aimed at increasing the life expectancy of road structures. In Canada, the network of paved public roads for two-lane-equivalent traffic is in excess of 400 thousand kilometres [1]; this is a distance that is ten times the Earth's circumference. In addition to enduring increasing traffic volumes, this vast road network is also exposed to some of the most extreme weather conditions: road surface temperatures in Canada can vary from 80°C in the summer to –50°C in the winter. As a result of these natural and man-made factors, the roads are deteriorating to the extent of becoming unravelled, cracked, or heaved; and they will require total reconstruction if surface preservation treatments are not made in time. With dwindling budgets and new federal regulations on materials, it is becoming increasingly difficult to maintain the integrity of the roads, creating a need to optimize our preservation materials.

Prompted by the "Possible Control Measures on VOCs Concentration Limits in Cutback Asphalt and Asphalt Emulsions" by Environment Canada [2], and the desire to migrate towards performance-graded emulsions, a greater understanding of the physical properties of asphalt emulsion residue is desired. Without understanding the underlying physics, it will be difficult to design optimal formulations for next-generation asphalt emulsions.

2.0 HIGH FLOATS

Within the broad anionic and cationic categories, there can be many different types of emulsions (based on the type of surfactant). One special type of anionic emulsion, which is the main focus of this research, is called the "high-float" emulsion.

High-float (HF) emulsions are dispersions of micron-sized asphalt droplets in water, with a special type of anionic surfactant functioning as a stabilizer. By allowing the water to evaporate from an HF emulsion, what remains is called a HF emulsion *residue*. Although indistinguishable in appearance from the original asphalt, the HF emulsion residue possesses rheological properties that are markedly different from those of asphalt.

HF emulsion systems are known to be especially immune to the problem of "bleeding." Bleeding, in the pavement industry, refers to the drainage of binder material (the asphalt) from the small spaces between the aggregates (see Figure 1). Such an effect will clearly reduce the structural integrity of an asphalt concrete and therefore must be avoided.

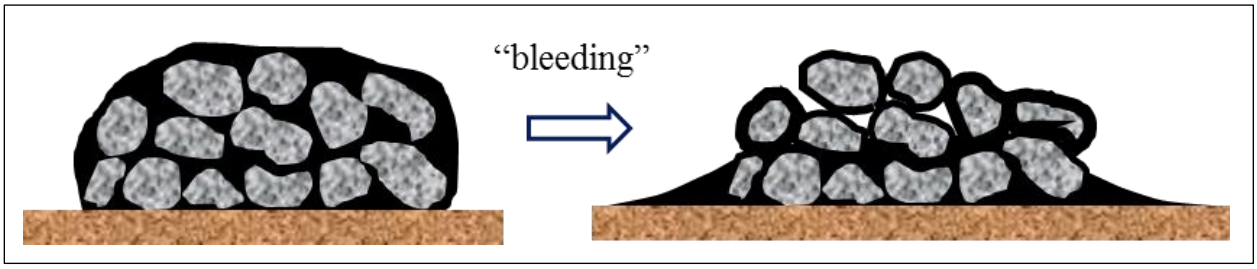

Figure 1. "Bleeding" of Asphalt Cement

The following order-of-magnitude analysis shows that capillary forces alone are not enough to hold the binder (assumed for now to be a liquid) in place: Suppose the asphalt has density, ρ and surface tension, γ. Let h be the thickness of the asphalt concrete layer, and a be the characteristic width of the spacing between the aggregates. If capillary action were the only mechanism of retaining the binder between the aggregates, then we must have Equation 1:

$$\rho g h \sim \frac{\gamma}{a} \quad \text{or} \quad a \sim \frac{\gamma}{\rho g h} \tag{1}$$

Putting in typical values of $\gamma \sim 10$ mN/m, $\rho \sim 10^3$ kg/m^3, $g \sim 10$ m/s^2, and $h \sim 1$ cm, we see that the spacing between the aggregates, a, must be of order 100 μm or smaller. In reality, this spacing is typically ~1 mm, which explains the bleeding effect in Figure 1 (assuming asphalt behaves as a liquid). Conversely, if bleeding is absent, it must be due to the presence of additional retaining forces within the binder material.

In regions where the road surface temperature can vary over a wide range, such as in Canada (from 80°C in the summer to −50°C in the winter), pavement construction is often faced with a dilemma: A "softer" asphalt should be used to prevent brittleness and cracking of the asphalt concrete at low temperatures, but the same binder will "bleed" at high temperatures due to its softness. The solution to this dilemma was proposed by K. E. McConnaughay in 1954 [3], who introduced a special type of anionic emulsion whose residue is resistant to bleeding in the summer and would not be overly brittle in winter; this emulsion has since been called HF emulsion. This peculiar name is derived from a rudimentary procedure known as the *float test* (ASTM D139); it was designed to quantify a binder's "consistency" [4]. Briefly, the test involves a floating dish of specific shape, size, material and weight. At the bottom of the dish is a hole, of a specific size, that is plugged with a binder material. The dish is next floated on a 60°C water bath, creating a hydrostatic pressure which pushes on the plugged hole (Figure 2).

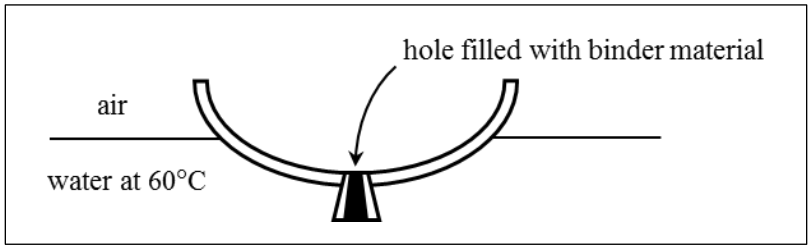

Figure 2. The Float Test (ASTM D139)

The time it takes for the 60°C water to break through the plugged hole is an indication of the binder's resistance to bleeding. Not surprisingly, "harder" asphalt would have a longer breakthrough time, which implies a lower tendency to bleed. These binders, unfortunately, are also the ones that become brittle and crack at sub-zero temperatures. Conversely, softer asphalts, which are designed to remain flexible at low temperatures, would (a) have very short water breakthrough times in float tests, and (b) lead to road surface bleeding at summer temperatures. An exception to this is the high-float emulsion. This is an emulsion that is formed using a special type of surfactant (discussed later). When subjected to the float test, the residue of such an emulsion shows a very long — or "high" — breakthrough time; it is for this reason that such emulsions are characterized as "high float." The rather arbitrary definition of an HF binder is one whose breakthrough time is 1,200 seconds or longer. In practice, this breakthrough time can often be indefinite. What is remarkable about HF emulsions is that it can be formed using any — including very "soft" — asphalt. By purposely choosing a soft asphalt (one which normally bleeds at

warmer temperatures) to form the droplets, the resulting emulsion residue would have the dual benefit of remaining resilient at cold temperatures and also does not bleed on hot summer days. It is for this reason that HF emulsions are a popular choice for Canadian road builders.

An HF asphalt emulsion is formed using a very specific type of anionic emulsifier (not all anionic emulsifiers can lead to HF quality). The emulsifier is a surfactant that is derived from the saponification of "tall oil" — a by-product from wood pulp mills. (The term "tall oil" comes from the Swedish word "talloja," which means pine oil. It is manufactured by the Kraft paper process which involves digestion of softwoods with caustic soda and sodium sulphides [5]. The process produces two waste components: rosin and fatty acids, which constitute the Crude Tall Oil, or CTO. Saponification of CTO at high pH would yield a tall oil soap, which is a water-soluble anionic surfactant.) In the pavement industry, it is often claimed that the tall oil soap, when used as emulsifier, can provide the emulsion residue with a "gel-like" quality. A clear demonstration of this gel-like effect is seen in Figure 3.

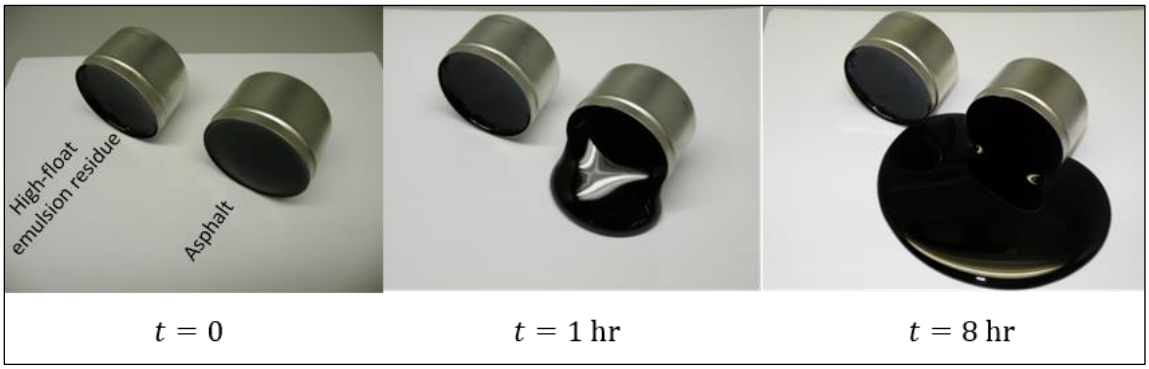

Figure 3. Flow behaviour of asphalt (right) and a high-float emulsion residue (left) formed from the same asphalt. The ambient temperature was 23°C.

The can on the right was filled with asphalt; its fluid behaviour was apparent as it slowly drained out of the container over a time scale of hours. The can on the left contained an emulsion residue formed from the same asphalt. Although the residue (i.e., what remained after the water component was evaporated from the emulsion) appeared identical to the original asphalt, its rheological behaviour was clearly different. In particular, the residue remained solid-like and showed no sign of deformation under gravity. It is noted that, in general, the "tipped can experiments" in Figure 3 correlate perfectly with the (almost equally primitive) float test: a binder that flows out of a tipped can would fail the float test (i.e., water breaking through in less than 1,200 seconds), while a "gel-like" material which remains in the can would lead to very long (or "high") breakthrough times.

Although the flow properties of an HF emulsion residue are unmistakably different from those of the original asphalt (as evident in Figure 3), what have been demonstrated so far are purely qualitative. At present, the only statements that one can make are: whether the material would flow out of a tipped can, and whether the water breakthrough time in a float test is longer than 1,200 seconds. To truly understand the science of HF emulsions, the following two questions must be answered:

1. What are the true rheological properties of a high-float residue?

2. How does the tall oil soap create these rheological properties?

3.0 YIELD STRESS

In many fields of engineering, practitioners have adopted technical terms that are less than precise. The road construction industry, for example, has for decades used terms such as "hard," "soft," and "gel-like" to characterize binder materials. Such adjectives, although descriptive, often lack in scientific rigour. One exception, however, is seen in a paper by Sutandar and Perrone [6], in which they attributed the "gel-like" behaviour of HF emulsion residues to a yield stress. The yield stress is a well-defined concept in rheology. A material that possesses an intrinsic yield stress will deform as a solid when the externally applied stress is below the yield level, and flow like a liquid when the external stress exceeds the yield [7]. Classic examples of materials with yield stresses are tooth paste and mayonnaise — neither will flow out of a container under its own weight. Although asphalt is a much "harder" material, it is mayonnaise (or tooth paste) that possesses a higher yield stress and, presumably, will be more resistant to bleeding.

Even though Sutandar and Perrone [6] had alluded to the possibility of a yield stress in HF emulsion residues, it was no more than a passing comment. A suggestion was made that the yield stress of an HF residue could be determined using the float test, but no further details were outlined.

4.0 PRINCIPLES OF RHEOLOGY – BRIEF OVERVIEW

4.1 Fluid and Solid Mechanics

Rheology concerns the flow and deformation of materials when they are subjected to external forces. The name "rheology" was first coined by Eugene Bingham, reportedly in the late 1920s [8]. Centuries before, however, there were already two branches of physics, known as fluid mechanics and solid mechanics, which accounted for such phenomena. Fluid mechanics describes how certain materials — specifically, viscous fluids — would flow under applied forces. The distinguishing features of a viscous fluid are:

- it can extend indefinitely when subjected to external load;
- it retains its deformed shape upon removal of the external load; and
- it possesses an inherent property — namely, viscosity — which limits the rate at which the material deforms.

Solid mechanics, on the other hand, is concerned with how certain materials — specifically, elastic solids — deform under applied forces. Distinguishing features of an elastic solid are:

- it undergoes finite (often small) deformation when loaded, with the deformation increasing monotonically with the load;
- it returns to its original shape when the external load is removed; and
- it exhibits effectively infinite rates of deformation.

Fluid mechanics and solid mechanics have enjoyed great successes in describing most materials, which surprisingly are well-approximated by one of the above "extreme" behaviours (i.e., elastic solid or viscous liquid). However, as technology advances, and especially as polymeric materials become more commonplace, it is apparent that there are many situations in which the substance in question behaves

neither as an elastic solid nor a viscous liquid; it shows some features of both. For example, some materials are fluid-like in that they can extend indefinitely, but exhibit partial recoils as the external forces are suddenly removed; other materials can "remember" their original configurations upon removal of external forces, but their rates of deformation are finite. Materials that show both viscous and elastic characteristics are said to be viscoelastic; it is the need to understand such materials that led to the science of rheology. In what follows, a brief summary of the principles of rheology will be given. The discussion will not include all detailed (and very mathematical) aspects of rheology and continuum mechanics, but be enough to provide a theoretical basis for this present work.

4.2 Stress and Strain

In rheology, material properties are specified by relations between stresses and strains (rather than between forces and displacements). For the present discussion, we focus only on stresses and strains that are associated with a specific mode of deformation known as pure shear.

Consider a small cubical element of the material that is under study. Pure shear occurs when equal and opposite forces are applied to two opposing faces of the element. It is important to note that these forces act only in tangential directions, i.e. no component of the force is normal to the surface on which it acts. A sketch of the situation is shown in Figure 4.

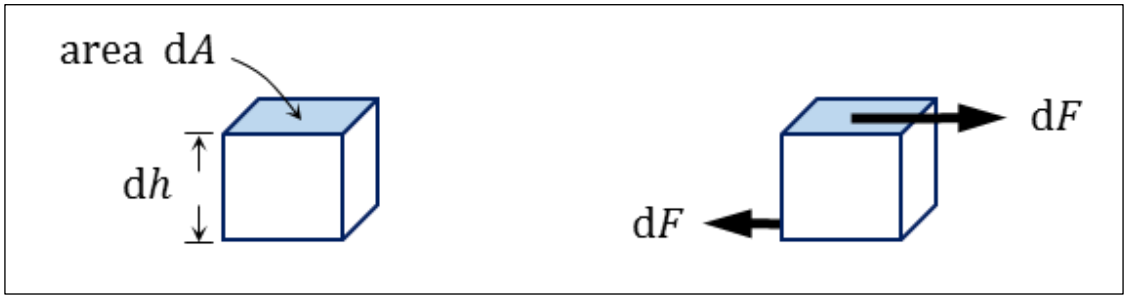

Figure 4. An elemental volume of material under pure shear. The differential forces, both of equal magnitude dF, act tangent to the surfaces.

As a result of this shearing, the material element will deform into a "parallelepiped"; this mode of deformation is described as pure shear. Figure 5 shows the front views of the differential element before and after deformation.

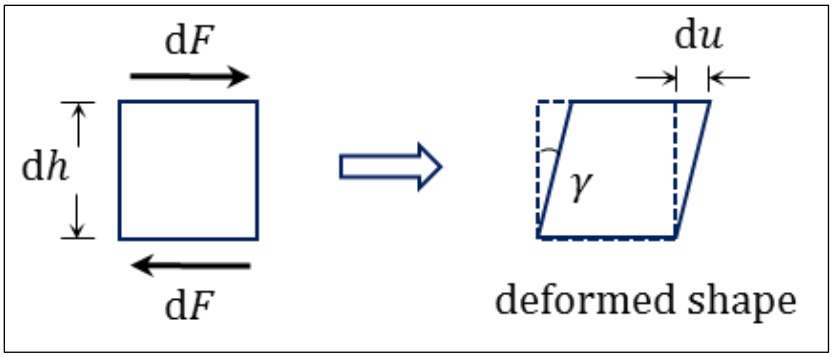

Figure 5. Front views of the material element before and after pure shear deformation.

The stress and strain components in a pure shear situation are defined in Equations 2 and 3:

Shear stress: $\sigma = \frac{\mathrm{d}F}{\mathrm{d}A}$ (units of N/m^2 or Pa) (2)

Shear strain: $\varepsilon = \frac{\mathrm{d}u}{\mathrm{d}h}$ (dimensionless) (3)

Since we deal exclusively with shear deformations in this work, we will omit the modifier "shear" from here on and refer to σ simply as the stress, and ε simply as the strain. (For small deformations, it is noted that the strain ε is equivalent to the angle γ shown in Figure 5; this is why shear strains are often represented as angles of deformation.)

4.3 Rheological Models

Having defined the stress σ and the strain ε, we now need mathematical relations that connect the two. Such relations, which are postulated based on empirical evidence, will describe how a material would deform or flow under applied stresses; these relations are often called rheological models. In what follows, the most common rheological models will be reviewed. In addition, based on our experimental results on high-float emulsion residues (see Results and Discussion), it is necessary to introduce here a new constitutive model that is a Bingham-like fluid with a "soft elastic yield stress" (discussed later).

4.3.1 Elastic Solid

The first rheological model is that for elastic solids (described at the beginning of this section). In the simplest case, when the stress is proportional to the strain, the material is called a Hookean solid; it follows the relation shown in Equation 4.

$$\sigma = G\varepsilon \tag{4}$$

Where the proportionality constant G is the shear modulus (units of Pa). It is noted that while Equation 4 represents the most common type of elastic behaviour, it is by no means unique. According to the criteria for an elastic solid, the material can follow any functional relationship between σ and ε, as long as (a) $\sigma = 0$ when $\varepsilon = 0$, and (b) the relation does not involve time derivatives of ε (i.e., rates of strain).

Figure 6a shows the 1-D metaphor of an elastic solid, which is depicted as a coil spring — with the spring force symbolizing the stress, and the spring extension symbolizing the strain.

4.3.2 Viscous Fluid

An elastic solid is one that offers resistance to deformation (i.e., ε), but not the rate of deformation (i.e., $\mathrm{d}\varepsilon/\mathrm{d}t$ can be effectively infinite). In contrast, a viscous fluid allows only finite $\mathrm{d}\varepsilon/\mathrm{d}t$, but offers no resistance to any amount of deformation. The simplest rheological model for a viscous fluid is the Newtonian fluid, with the stress-strain relation given by Equation 5.

$$\sigma = \mu\,\dot{\varepsilon} \tag{5}$$

Where $\dot{\varepsilon}$ is the shorthand notation for $\mathrm{d}\varepsilon/\mathrm{d}t$ (the rate of strain), and μ is the viscosity (often constant for a given temperature, with units of Pa·s).

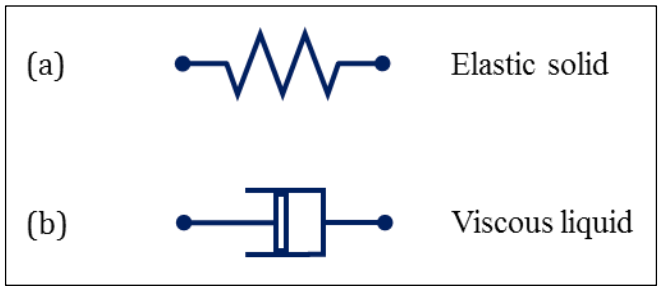

Figure 6. One dimensional metaphors of elastic solids and viscous fluids.

Viscosity is a mechanism that limits the rate of deformation through conversion of mechanical energy into heat. Unlike in the case of elastic solids, this mechanical energy cannot be recovered and is said to be dissipated. The 1-D metaphor for a viscous liquid is often depicted as a dashpot (see Figure 6b), with the tension in the device again symbolizing σ, and the amount of axial extension symbolizing ε.

The Hookean solid and Newtonian liquid are the basic rheological models in the fields of solid mechanics and fluid mechanics, respectively. There are, however, many other materials that do not follow these two "extreme behaviours." Some of the more common examples are discussed in the following sections.

4.3.3 Kelvin-Voigt Solid

This type of material is classified as a solid as it can "remember" its original shape; i.e., it always recoils back to its original configuration upon removal of external forces. However, unlike purely elastic bodies, the rates of deformation of a Kelvin-Voigt material are not infinite; this suggests there is internal dissipation within the material. When subjected to a sudden external load, the material will not deform instantaneously (as does an elastic substance), but will approach its new configuration in a time-dependent (exponential-like) manner. The simplest way to represent such behaviours is to have an elastic element acting in parallel with a viscous counterpart, as shown in Figure 7.

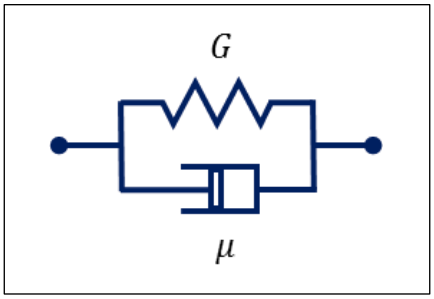

Figure 7. Representation of a Kelvin-Voigt material.

Since the two elements act in parallel, the stress in a Kelvin-Voigt material is the sum of the elastic and viscous contributions, as shown in Equation 6.

$$\sigma = G\varepsilon + \mu\dot{\varepsilon} \tag{6}$$

where G and μ are the shear modulus and the viscosity, respectively.

4.3.4 Maxwell Fluid

This is a material that flows like a liquid under constant applied force, but exhibits partial recoil when the force is suddenly removed. If subjected to a sudden external load, the Maxwell fluid can deform instantaneously; this aspect is similar to an elastic solid. However, unlike a solid, if the level of strain in a Maxwell fluid is maintained at a fixed level, one will see a gradual (exponential-like) relaxation of the stress within the material; this continues until σ reaches zero. To model such behaviours, Maxwell, in 1867, suggested putting an elastic element in series with a viscous element, as shown in Figure 8 [9].

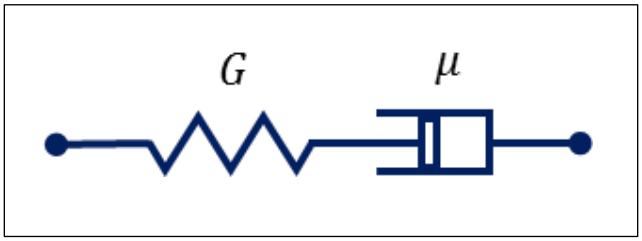

Figure 8. Representation of a Maxwell material.

The mathematical model requires that there be two measures of strain within a Maxwell material; these are ε_e and ε_v, which are the strains associated with the elastic element and the viscous element, respectively. Since the elements are in series, the total strain in the material is simply the sum of the two internal parts, as per Equation 7.

$$\varepsilon = \varepsilon_e + \varepsilon_v \tag{7}$$

Also, the serial arrangement means that the elastic and viscous stresses must be equal, as per Equation 8.

$$\sigma = G\varepsilon_e = \mu\dot{\varepsilon}_v \tag{8}$$

Combining equations 7 and 8, one obtains Equation 9.

$$\dot{\varepsilon} = \frac{\dot{\sigma}}{G} + \frac{\sigma}{\mu} \tag{9}$$

Where the dots above ε and σ represent differentiations with respect to time.

4.3.5 Materials with Yield Stress

There is another major class of materials that does not fit any of the previous descriptions. These are materials that possess a yield stress σ_y, with the following unique features:

- When the magnitude of the applied stress is below σ_y, the material behaves as a solid.
- When the magnitude of the applied stress exceeds σ_y, the material flows like a liquid.

Many substances (e.g. toothpaste, mayonnaise, and HF emulsion residue) fall into such a category. In the literature, the most general model for materials with yield stresses is the Herschel-Bulkley fluid [6], which is a three-parameter empirical relation of the form shown in Equation 10.

$$\left.\begin{array}{l}\text{when } \sigma < \sigma_y: \quad \dot{\varepsilon} = 0 \\ \text{when } \sigma > \sigma_y: \quad \sigma - \sigma_y = K(\dot{\varepsilon})^n\end{array}\right\} \tag{10}$$

Where K is the so-called "consistency coefficient" and n is the "flow index." When n = 1, the model reduces to the well-known Bingham plastic, for which the shear rate $\dot{\varepsilon}$ is proportional to the excess stress $\sigma - \sigma_y$. If n = 1 and σ_y = 0, the material becomes a Newtonian fluid.

It is noted here that the Herschel-Bulkley model (Equation 10) does not provide a complete description of the rheological behaviour: when $\sigma < \sigma_y$, the material should be allowed to deform as a solid (i.e., with non-zero ε), but the elastic stress-strain relation is not specified in Equation 10. To avoid introducing more empirical parameters, most researchers assume the material to be completely rigid (i.e., ε = 0) when the applied stress is below the yield point. This, as we will see in the results, fails to capture important features of experimental observations. In this work, we propose a new three-parameter model (an alternative to the Herschel-Bulkley fluid) for materials that exhibit yield stresses. In our model, the exponent n (associated with viscous dissipation) is fixed at 1; that is, we are neglecting shear-thinning and shear-thickening effects. A new elastic parameter will be added to describe the deformation in the regime $\sigma < \sigma_y$. Our new rheological model is given by Equation 11.

$$\sigma = \sigma_e + \mu\dot{\varepsilon} \tag{11}$$

Where σ_e is the elastic stress, which is a function only of the strain ε. Equation 11 appears very similar to the Kelvin-Voigt model (Equation 6). This similarity in fact points to a subtle but important point: If elastic deformations were allowed below the yield point, one must be careful to not treat the material as purely elastic (implying infinite shear rates). Instead, the material should respond to time-varying excitations in the fashion of a Kelvin-Voigt solid — with finite rates of deformation. Further, the rate-limiting viscosity below the yield point should be the same as that when the yield stress is exceeded. What differentiates Equation 11 from a Kelvin-Voigt solid is that the elastic stress in this case has two parameters: an elastic modulus G that determines the initial deformation, and a yield stress σ_y that provides a "ceiling" to the elastic stress (both parameters have units of Pa). The most straightforward way of expressing σ_e in terms of ε is as shown in Figure 9a and described by Equation 12a.

$$\sigma_e = \begin{cases} G\varepsilon; & \varepsilon < \sigma_y/G \\ \sigma_y; & \varepsilon > \sigma_y/G \end{cases} \tag{12a}$$

An alternative form for the elastic stress σ_e, which involves also only two parameters, is shown in Figure 9b. Here, the elastic function has an initial slope G, which is followed by an exponential (asymptotic) approach to the maximum stress level. In this case, the functional form for σ_e is per Equation 12b.

$$\sigma_e = \sigma_y\left[1 - \exp\left(-G\varepsilon/\sigma_y\right)\right] \tag{12b}$$

The elastic function in Figure 9b (and Equation 12b) represents a "softer" elastic response compared to that in Figure 9a.

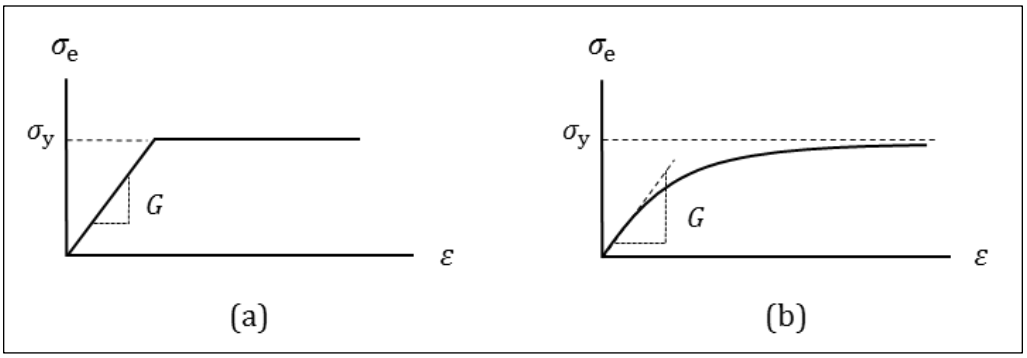

Figure 9. The two possible forms of the elastic function σ_e (ε) that appears in equation 11. The functional forms in (a) and (b) are given by equations 12a and 12b, respectively. Both are two-parameter functions, and the elastic stress in case (b) represents a "softer" response.

It will be seen in the Results section that the elastic stress shown in Figure 9b provides a much better rheological model for the high-float residue — and most likely also for other materials that exhibit yield stresses. (There is no reason why internal structures which give rise to yield stresses should suddenly "switch off," as depicted in Figure 9a.)

4.4 Stress-Ramp Excitation

Oscillatory excitations (from which one obtains storage and loss moduli) are appropriate only for linear materials. For materials with inherent yield stresses, a more suitable type of excitation is the stress-ramp, which is a linear increase (or ramping-up) of the external stress with time, as per Equation 13.

$$\sigma(t) = \alpha\, t \tag{13}$$

Where α is the constant ramp rate (units of Pa/s). Such an excitation is aimed specifically at materials with inherent yield stresses. The expectation is that when the applied stress reaches the material's yield point, there will be obvious (and perhaps discontinuous) changes to the physical observables. The observable that is most commonly reported in stress-ramp experiments is the apparent viscosity μ_{app} ; it is defined simply in Equation 14.

$$\mu_{\text{app}} = \sigma/\dot{\varepsilon} \tag{14}$$

Apparent viscosity is often plotted against the applied stress (i.e. μ_{app} vs σ, with the latter given by Equation 13). Note that although μ_{app} appears to be a viscosity, it may not be due to any dissipative mechanism at all. For example, if a stress-ramp were applied to a Hookean solid, it is easy to show that $\mu_{\text{app}} = Gt$, i.e. the apparent "viscosity" increases linearly with time, even though the material is in fact purely elastic and involves no dissipation of energy.

Based on stress-ramp data, plotting μ_{app} vs σ can be a very clear way of separating elastic and viscous effects. It is a simple exercise to show that for (a) a Hookean solid, (b) a Newtonian fluid, and (c) a Bingham plastic, the μ_{app} vs σ relations are as depicted in Figure 10. In the case of Bingham plastic, the material is assumed rigid below the yield point, which leads to infinite apparent viscosity for $\sigma < \sigma_y$.

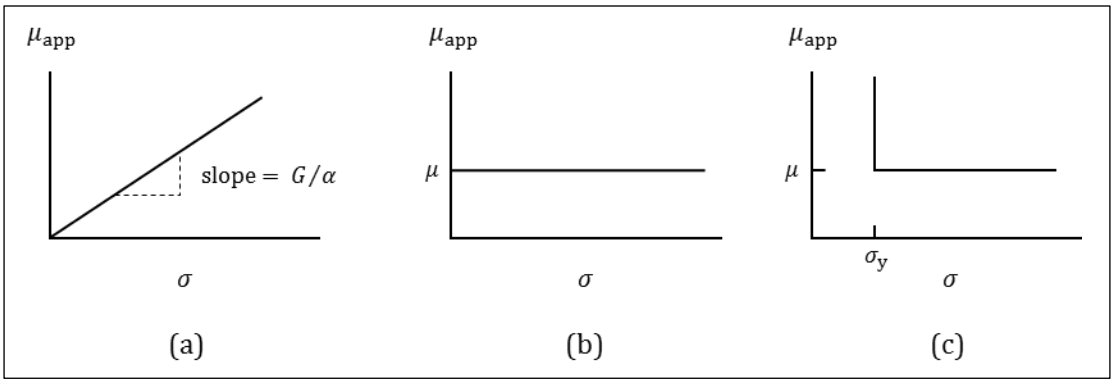

Figure 10. Variations of the apparent viscosity μ_{app} with the applied stress σ; the latter is ramped up linearly with time according to equation 13. The three responses are for (a) a Hookean solid, (b) a Newtonian liquid, and (c) a Bingham plastic that is rigid below its yield point.

For materials with more complex rheology, it is very difficult (if not impossible) to determine analytically their responses to stress-ramp excitations. In this work, numerical simulations will be used. Since stress-ramp experiments are intended specifically for materials with yield stresses, we will focus on the two rheological models that we proposed earlier in Equations 12a and 12b. Figure 11 shows a simple Euler-type algorithm that is used here to calculate the responses of such materials. Results of this simulation will be discussed in Section 6.

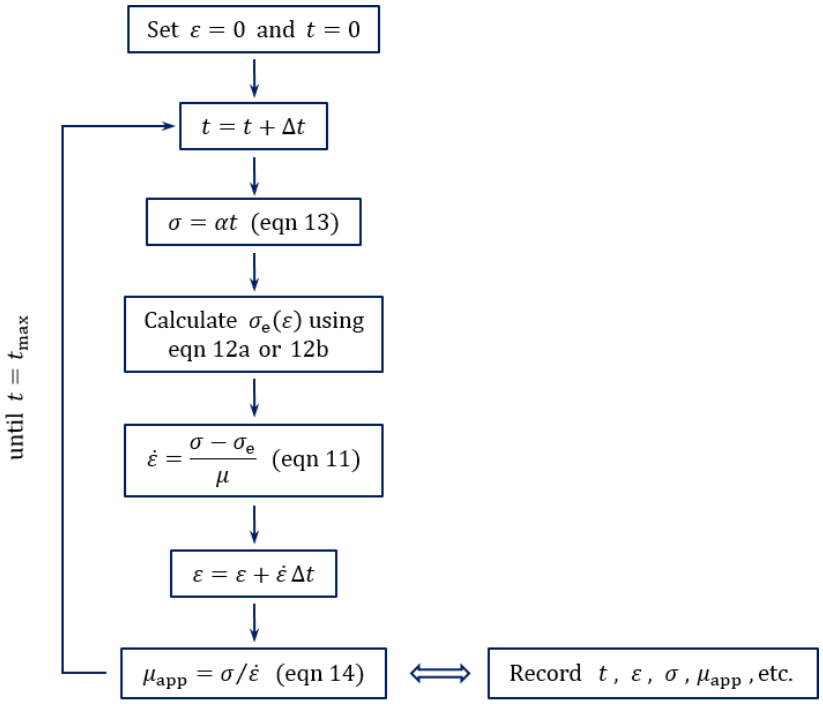

Figure 11. Simple algorithm for calculating the response of a material to stress-ramp excitation. The material possesses an inherent yield stress according to Equations 11 and 12.

5.0 MATERIALS AND METHODS

The rheological experiments in this research, including the float test and dynamic shear rheometry, were conducted at Gecan, a division of Canadian Road Builders Inc. located in Acheson, Alberta. The following is a summary of the procedures involved in sample preparation and testing.

5.1 Materials

5.1.1 Selected Binders

Only three types of samples were prepared and subjected to experimentation. The intention here was to focus on the least number of samples that would provide the maximum amount of information and insight. The three materials that were tested were all binders, i.e., the glue that holds together the aggregates in an asphalt concrete (see Figure 1). The three binders were:

Binder 1: Asphalt

In all subsequent discussions, we will refer to this material simply as "asphalt." To be specific, however, this is a special grade of asphalt known as PG 58-28. The designation suggests that the asphalt has certain required physical properties in the temperature range of +58°C to –28°C [10]. This particular grade of asphalt was chosen for the present study due to its common usage throughout Alberta — in both road rehabilitation and construction of new pavements. PG 58-28 can be used in a hot-mix process (i.e., liquefaction of asphalt by heating) or can form the dispersed phase of an emulsion. It is noted that the asphalt in Figure 3 — the material the flowed out of the tin can — was PG 58-28.

Binder 2: Residue A

This is the residue of an HF emulsion. The proper designation of the emulsion is HF-100S; it is commonly used in Canada for road preservation and rehabilitation. The residue of HF-100S (called "Residue A" in this paper) is often the binder of choice due to its resistance to "bleeding." Most importantly for this study, Residue A is formed from the same asphalt as Binder 1 (i.e., PG 58-28). It is noted that the emulsion residue in Figure 3 — the material that remained in the tin can — was Residue A. This simple demonstration alone is clear evidence that, contrary to common belief, an emulsion residue may not necessarily have the same material properties as the original asphalt.

Binder 3: Residue B

Unlike the two former binders, this material is not used in real pavement applications. Residue B is similar to Residue A in every respect, except that it is formed with only half of the surfactant dosage. The reason we study such a material is because it is somewhat of a "halfway point" between pure asphalt (PG 58-28, which is prone to bleeding) and Residue A (HF-100S residue, which is resistant to bleeding). As such, Residue B provides an important intermediate case for the fundamental understanding of high-float emulsions.

The compositions of the three binders are provided in Table 1.

For the emulsions of Residue A and Residue B, the water component was adjusted to pH 12 with NaOH. Such a high pH was necessary to saponify the CTO and allow the release of anionic surfactants into the aqueous phase.

Table 1. Composition of samples subjected to experimentation.

	Asphalt (PG 58-28) wt%	Water wt%	Crude Tall Oil (surfactant) wt%
Asphalt	100	-	-
Residue A's emulsion	62	35.8	2.2
Residue B's emulsion	62	36.9	1.1

5.1.2 Creation of an Asphalt Emulsion

In addition to CTO surfactants, which function as emulsifiers, mechanical energy must also be supplied to create an asphalt emulsion. This was done with the aid of a colloidal mill, which is a high shear flow device with an adjustable gap size between its rotor and stator, along with a variable speed drive to control the shear rate — and ultimately the size of the asphalt droplets. The laboratory colloidal mill used in this study was a Dalworth mill. Constructed with a Baldor-Reliancer 5-hp motor, the mill has the capability of rotating at 3,450 rpm, creating the necessary mechanical energy to disperse the PG 58-28 asphalt into micron-sized droplets in an aqueous medium. Before being injected into the colloidal mill, the asphalt temperature must be raised to a minimum of 135°C to decrease its viscosity. The final temperature of the emulsion should, however, be below 100°C to avoid boiling and foaming of the mixture.

5.1.3 From Emulsion to Residue

With the focus of this study primarily on the residue of HF emulsions, it is important to note the equipment and procedures associated with obtaining emulsion residues. Currently, there are several accepted methods — the most notable being residue by distillation (ASTM D6997/AASHTO T59) testing standards [11, 12]. The American Association of State Highway and Transportation Officials (AASHTO) describes this method as a "quantitative determination of residue and oil distillate in emulsified asphalt for specification acceptance, service evaluation, control, and research [12]." There are also numerous accepted and proposed methods outlined in the Transportation Research Circular No. E-C122 from 2007, e.g., residue by evaporation (D6934/T59), weathering rack, thermostatically-controlled hot plate, dehydrator and Stirred Air Flow Test (SAFT) with nitrogen, to name a few [13]. For the present study, residue by distillation was used to obtain the emulsion residues (i.e., Residues A and B).

This protocol requires measuring 200 grams of emulsified asphalt into a still, so that the water component can be removed through evaporation. The duration of the process is approximately one hour and reaching a temperature of 260°C. Distillation is an effective and rapid means of acquiring sufficient residual sample to carry out various tests. As mentioned earlier, although the emulsion residue and the original asphalt are indistinguishable in appearance, they may possess fundamentally distinct rheological properties (as evident in Figure 3). The following section provides descriptions of the various methods that were used in this study to probe the rheological properties of the three binders that were mentioned earlier in this section.

5.2 Methods

Two instruments — one rather simple and the other sophisticated and versatile — were used in this study to test the binder materials. The simple instrument is the float test dish that was illustrated in Figure 2; its specific dimensions and related details are summarized in ASTM D139. The sophisticated instrument is

the Dynamic Shear Rheometer (DSR); the make and model of the device are: TA Instruments, Discovery HR-1 Hybrid Rheometer.

The DSR is capable of applying time-varying excitations, in pure shear mode, to a binder sample. The time-varying excitation can be programmed to be of any arbitrary form. In this work, however, we will limit our focus to stress-ramp excitations. The following are the two tests that were performed on the binder materials:

Experiment	Instrument	Description
Float test	Float test dish	Determine water breakthrough time (see Figure 2). Material is deemed "high float" if breakthrough time exceeds 1,200 seconds.
Stress-ramp	DSR	Fix $T = 58°C$; ramp up stress σ linearly with time according to Equation 13. Measure μ_{app} (Equation 14) as function of σ.

6.0 RESULTS AND DISCUSSION

6.1 Float Test

This simple experiment, designed to measure the "consistency" (a term which has no real rheological meaning) of a binder material, actually provides invaluable guidance to subsequent investigations. Specifically, semi-quantitative results from float tests can give strong hints of whether a material possesses a yield stress — and hence its ability to resist bleeding. Following the exact ASTM D139 procedures, the three binder samples exhibited water breakthrough times as shown in Table 2.

Table 2. Float Test Results

Binder	Breakthrough Time (s)
Asphalt	35
Residue A	>1,200 (effectively indefinite)
Residue B	425

The strong contrast is between pure asphalt (the PG 58-28) and Residue A — as HF residue formed from droplets of the same asphalt. The fact that Residue A showed an indefinite breakthrough time suggests that its "consistency" is not viscosity-based; it is more likely due to an elastic resistance to deformation. This elasticity, however, cannot be Maxwell-like in that it is connected in series to a viscous element (see Figure 8) since a Maxwell material is capable of unlimited deformation and will therefore fail the float test. The elastic resistance inherent in Residue A must therefore be more akin to Kelvin-Voight-type behaviour (Figure 7) as such a material, with its elastic element acting in parallel with dissipation, will allow only finite deformation (and hence maintaining the caulking at the bottom of the floating dish). Residue B, based on the float test results, appears much more similar to pure asphalt than to Residue A. This is an interesting observation, as Residue B's composition is almost identical to that of Residue A —

except for a reduced amount of surfactants that was used. (Note that the surfactant dosages for Residues A and B were both in trace amounts, but apparently there is a significant difference between "trace amount" and "50 percent of trace amount").

6.2 Stress Ramp

Details of the stress-ramp experiment were discussed in Section 4.3. The procedure involves applying a constantly-increasing stress to a material that is suspected of having a yield stress. When the applied stress reaches the yield value, there will be an obvious, and perhaps discontinuous, change in the apparent viscosity μ_{app} (see Equation 14). It is also worth repeating one of the conclusions from Figure 10: if the sample were a true Newtonian liquid that does not have a yield stress, we would see $\mu_{\text{app}} = \mu$ = the true viscosity of the material.

Figure 12 shows the stress-ramp responses of the three binder materials. The temperature was 58°C, and the ramp rate (α in Equation 13) was 100 Pa over a period of 1 hour. The asphalt curve showed a constant — and the lowest — value of μ_{app} at 140 Pa·s; this is in fact the true viscosity of the substance. The "flatness" of the asphalt curve indicates that this binder does not possess a yield stress. Similarly, the Residue-B curve is essentially level at $\mu_{\text{app}} \approx 220$ Pa·s. This leads one to speculate that Residue B, like asphalt, does not have a yield stress, and that it is essentially a Newtonian liquid with a viscosity of roughly 220 Pa·s. Interestingly, both asphalt and Residue B had failed the float test (Section 6.1). By contrast, the Residue-A curve shows an obvious peak at $\sigma = 22$ Pa.

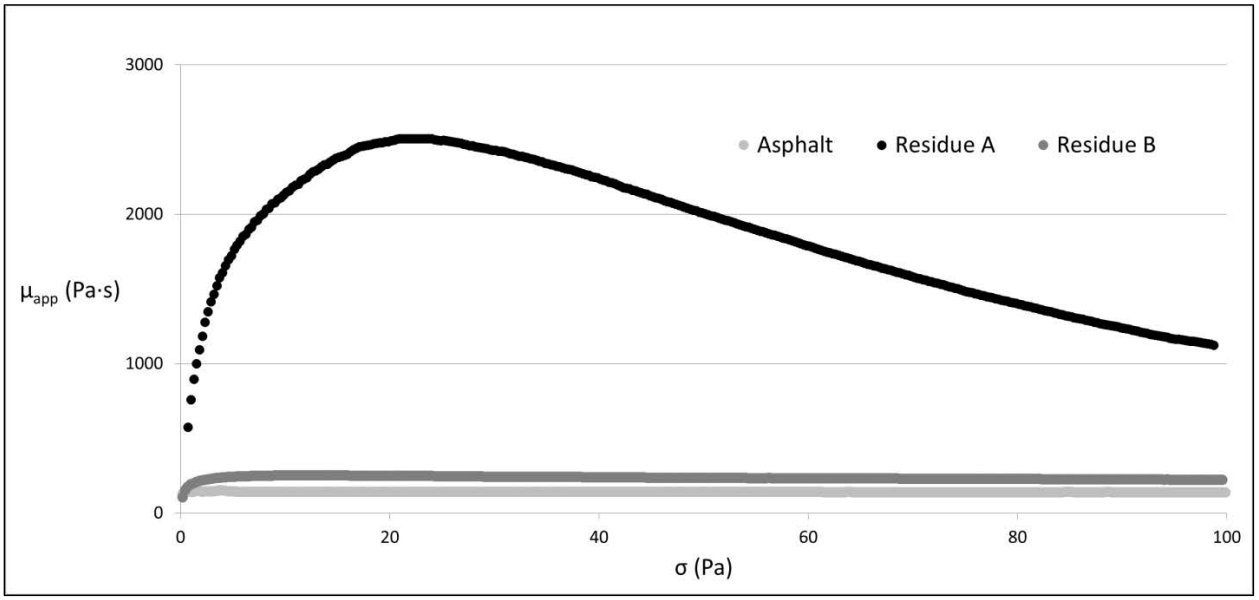

Figure 12. Stress-Ramp Responses

As will be shown, such a value can be interpreted as a rough measure of the yield stress. It should also be noted that the very large μ_{app} value for Residue A (up to 2,500 Pa·s) is not a real viscosity: As seen in Figure 10a, when a Hookean solid is subjected to stress-ramp excitation, the *apparent* viscosity is expected to rise linearly with the applied stress, even though the material has in fact no viscous dissipation at all. This leads one to suggest that, in the case of Residue A, the initial rapid rise in μ_{app} is due not to

dissipation, but to an inherent elasticity of the material. As σ reaches the yield value, this elastic contribution subsides and hence the resulting decrease in μ_{app}.

From this discussion, it is seen the stress-ramp response curve (i.e. μ_{app} vs σ) can be very informative. In particular, one can conclude that:

- Asphalt (i.e. PG 58-28) is a Newtonian liquid with μ = 140 Pa·s;
- Residue B is essentially a Newtonian liquid with $\mu \approx$ 220 Pa·s; and
- Residue A is a complex fluid with a yield stress σ_{y} of roughly 22 Pa.

Identifying the yield stress from a μ_{app} vs σ curve is straightforward — one simply needs to locate the peak. However, there are other (more subtle) properties of a yield-stress material, such as the elastic modulus, which should also be determined (see Equations 11 and 12). To further understand these subtle features would require detailed numerical modelling.

6.3 Numerical Simulation

With the aid of a computer, it is straightforward to simulate the stress-ramp curve — provided a rheological model is given. In Section 4.3.5, we proposed two such models for yield-stress materials. These models are specified by Equations 12a and 12b; the elastic stresses associated with these models are illustrated in Figure 9. Both these models involve three parameters: the yield stress σ_{y}, the elastic modulus G, and the viscosity μ. In addition, the stress ramp rate α must also be specified. Given these values, the stress-ramp response can be calculated using the algorithm shown in Figure 11.

After some trial simulations, it became clear that the first yield-stress model — the one whose elastic stress is illustrated in Figure 9a — is completely unrealistic. The second yield-stress model, with the "softer" elasticity as shown in Figure 9b, provides a much better approximation to the observed trend. As demonstration, we will show two simulations based on the following parametric values:

σ_{y} = 30 Pa; G = 6 Pa; μ = 500 Pa·s; and α = (100 Pa)/(3600 s)

First, using the elastic stress according to Equation 12a (and illustrated in Figure 9a), we have the stress-ramp response shown in Figure 13.

Comparing this calculated curve with the Residue-A curve in Figure 12, it is clear that this rheological model is unrealistic. The problem is due to the discontinuous change in elastic modulus (i.e., slope of the σ_{e} vs ε curve in Figure 9a), which leads to the pointed peak in Figure 13. In contrast, the elastic model according to Equation 12b (and illustrated in Figure 9b) produced the simulation shown in Figure 14.

Although not precisely identical to the Residue-A curve in Figure 12, the "softer" elastic model represents a significant improvement over what is shown in Figure 13. It is noted that this improvement was not made at the expense of additional parameters — both models involved three fitting values.

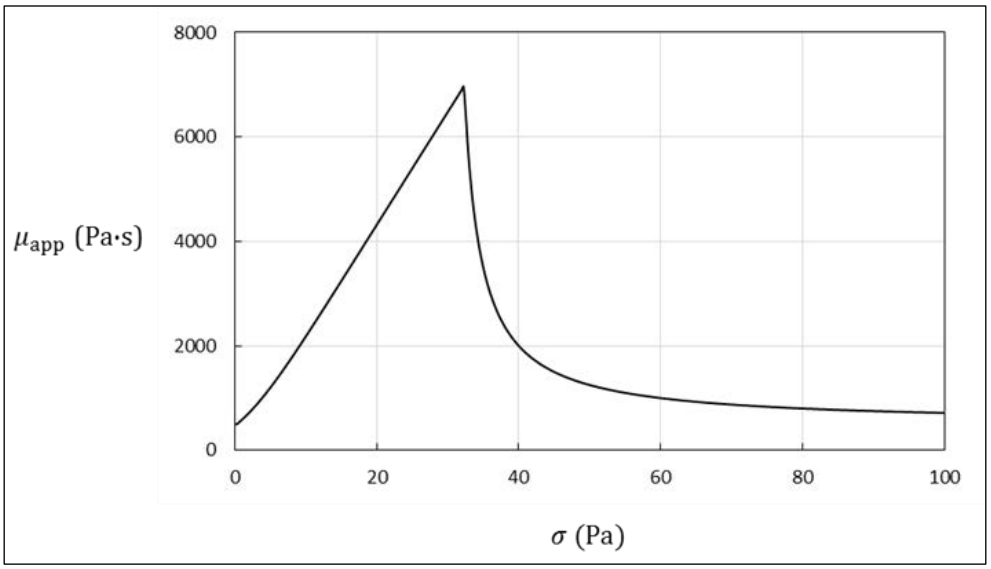

Figure 13. Numerical simulation of stress-ramp response according to Equations 11 and 12a.

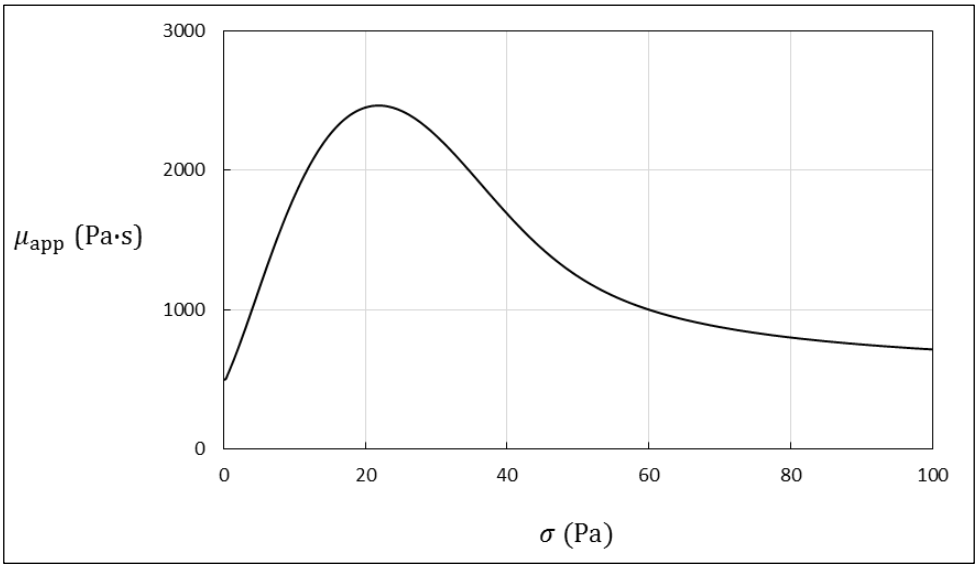

Figure 14. Numerical simulation of stress-ramp response according to Equations 11 and 12b.

6.4 Speculation on the Microstructure of HF Residue

We have thus far proposed a novel rheological model for the HF residue. The most important feature of the model is the existence of a yield stress, below which the material deforms elastically as a soft (i.e. non-Hookean) material. Despite being borne out by empirical evidence, the model remains phenomenological. True understanding of HF residues — and the design of improved emulsion systems — cannot be achieved without knowing the underlying mechanism(s) which lead to the observed rheology. Unfortunately, our research is at present still at its early stages; we can therefore only speculate on the "internal workings" of this unique material. We begin by discussing the *microstructure* of an HF residue.

The common belief is that, as water evaporates from an asphalt emulsion, the small oil droplets will recombine and return to being the original asphalt material. What is implicitly assumed in this scenario is that the asphalt droplets will *coalesce*, resulting, in effect, in a final asphalt "drop" that is as large as the residue itself. If this were the case, the residue would deform and flow just as would the original asphalt (the trace amount of emulsifier that remains in the residue cannot possibly give rise to the material's elastic resistance to flow). The situation in Figure 3 clearly contradicts the "coalescence theory." We believe that, instead of coalescing, the asphalt droplets would *coagulate* while retaining each droplet's individuality. As evidence, Figure 15 shows what has remained on a microscope slide as a small amount of an HF emulsion was left to dry. Within the remnant patches, it is clearly seen that the asphalt droplets have *coagulated but not coalesced*. These patches, we believe, are "microcosms" of the HF residue.

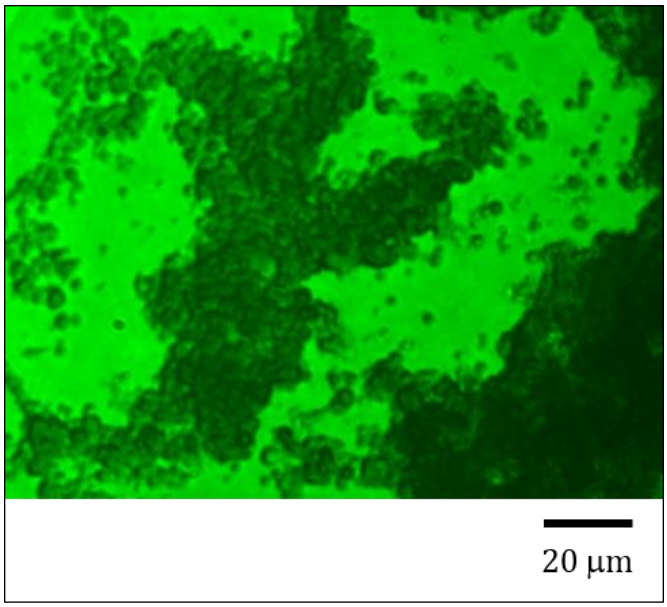

Figure 15. What remains on a glass surface as a small amount of high-float emulsion was left to dry.

We propose the following: The microstructure of an HF residue is one that consists of many coagulated (but un-coalesced) asphalt droplets. These coagulated droplets can conceivably trap small amounts of water in between them. Indeed, initial moisture analysis (by Karl Fischer titration) has shown that there are trace amounts of water within the HF residue — roughly 100 ppm. The granulated nature of the HF residue provides a ready explanation for the existence of a yield stress: it requires a certain amount of threshold force to overcome the interlocking between the granules (the droplets) [14]. Moreover, once the yield stress is exceeded and the material begins to flow, it is the friction between the droplets — and not the natural viscosity of asphalt — that determines the macro-scale viscosity of the residue. As support for this, the estimated viscosity of the HF residue was 500 Pa·s (see Section 6.3), which is quite different from the natural viscosity of asphalt (140 Pa·s) at the same temperature.

We have *speculated* on the microstructure of the HF residue, and how this microstructure could give rise to a yield stress. This, however, does not constitute a definitive understanding of the HF system. More in depth studies are needed to confirm the microstructure of HF residue. In addition, it is essential to understand the origin and magnitude of the colloidal forces which prevent the asphalt droplets from coalescing, and how these forces are related to the nature of the emulsifiers. Many critical questions regarding the fundamental science of HF emulsions remain unanswered.

7.0 CONCLUSIONS AND FUTURE WORK

We have demonstrated that the high-float emulsion residue (Residue A) has rheological properties that are completely different from those of the original asphalt (PG 58-28). Most importantly, the material possesses a yield stress which can prevent the "bleeding" problem that was illustrated in Figure 1. The yield stress of a high-float residue is estimated to be about 22 Pa. We have also proposed a new rheological model (Equations 11 and 12b) which best captures the flow properties of the high-float emulsion residue.

This research has made significant contributions toward understanding the rheology of high-float residues. In addition to proposing a new yield-stress model, we have also demonstrated that a simple protocol — the stress-ramp excitation — can be used to determine yield stress values. With further development, such a procedure can have the potential of replacing the traditional float test (ASTM D139).

In the future we hope to conduct stress-ramp excitations on multiple high-float emulsion grades from various suppliers, expand our rheological modeling, and provide further correlation between yield stresses and microstructures.

In conjunction with industrial developments, research on the fundamental science of emulsions is needed to better design "next-generation" high-float products.

REFERENCES

[1] Transport Canada. "Road Transportation", https://www.tc.gc.ca/eng/policy/anre-menu-3021.htm (April 7, 2016).

[2] Environment Canada. "Possible Control Measures on Volatile Organic Compounds (VOC) Concentration Limits in Cutback Asphalt and Emulsified Asphalt – Discussion Paper and Considerations for the Development of Possible Control Measures," Report En14-81/2013E-PDF, Gatineau, Quebec (2012).

[3] McConnaughay, K. "Asphaltic Paving Composition", US Patent 2,855,319. United States Patent Office (1958).

[4] ASTM International (ASTM) D139-12. "Standard Test Method for Float Test for Bituminous Materials", Annual Book of ASTM Standards, Road and Paving Materials; Vehicle-Pavement Systems, 04.03, West Conshohocken, Pennsylvania (2012).

[5] Johnson RA, Juristovski AG. "Physical Properties of Tall Oil Pitch Modified Asphalt Cement Binders", Physical Properties of Asphalt Cement Binders, STP 1241, American Society for Testing and Materials (ASTM), Philadelphia, Pennsylvania, 214-231 (1995).

[6] Perrone P, Sutandar T. "High Float Emulsified Asphalt; It's Properties, and Applications", Proceedings, Canadian Technical Asphalt Association, 25, 80-107 (1980).

[7] Steffe JF. Rheological Methods in Food Processing Engineering, Freeman Press, East Lansing, Michigan (1996).

[8] Reiner M. "The Deborah Number", Physics Today, 17 (1), 62 (1964).

[9] Malkin AY, Isayev A. Rheology: Concepts, Methods and Applications (2nd ed.), ChemTec Publishing, Toronto (2012).

[10] McGennis RB, Shuler S, Bahia HU. "Background of SUPERPAVE Asphalt Binder Test Methods", Report No. FHWA-SA-94-069, Federal Highway Administration, Washington, D.C. (1994).

[11] ASTM International (ASTM) D6997-12. "Standard Test Method for Distillation of Emulsified Asphalt", Annual Book of ASTM Standards, Road and Paving Materials; Vehicle-Pavement Systems, 04.03, West Conshohocken, Pennsylvania (2012).

[12] American Association of State Highway and Transportation Officials T59-05. "Standard Test Method for Emulsified Asphalts", Standard Specifications for Transportation Materials and Methods of Sampling and Testing, Part 2A, 2012 Edition, Washington, D.C. (2012).

[13] Asphalt Emulsion Technology. Review of Asphalt Emulsion Residue Procedures. Transportation Research Circular No. E-C122, Transportation Research Board, National Research Council, National Academies, Washington, D.C. (2007).

[14] Coussot P, Raynaud JS, Bertrand F, Moucheront P, Guilbaud JP, Huynh HT, Jarny S, Lesueur D. "Coexistence of Liquid and Solid Phases in Flowing Soft-Glassy Materials", Phys Rev Lett, 88 (21) 218301 1-4 (2002).